Applied Surface Science 258 (2012) 9891–9895

Contents lists available at SciVerse ScienceDirect

Applied Surface Science

journal homepage: www.elsevier.com/locate/apsusc

The structural and optoelectronic properties of Ti-doped ZnO thin films prepared by introducing a Cr buffer layer and post-annealing

Y.C. Lin [a], C.Y. Hsu [b], S.K. Hung [a], C.H. Chang [b], D.C. Wen [c,*]

[a] Department of Mechanical Engineering, National Chiao Tung University, Taiwan, ROC
[b] Department of Mechanical Engineering, Lunghwa University of Science and Technology, Taiwan, ROC
[c] Department of Mechanical Engineering, China University of Science and Technology, Taiwan, ROC

ARTICLE INFO

Article history:
Received 9 May 2012
Received in revised form 11 June 2012
Accepted 14 June 2012
Available online 23 June 2012

Keywords:
Ti-doped ZnO
Buffer layer
Post-annealing
Magnetron sputtering
Electrical resistivity
Transmittance

ABSTRACT

This work investigates the effects of Cr buffer layers and post-annealing on the properties of titanium-doped zinc oxide (TZO) thin films prepared by radio frequency magnetron sputter. All films had a (0 0 2) preferential orientation along the *c*-axis at $2\theta \sim 34^{\circ}$. The crystallinity, grain size, Hall mobility and carrier concentration of TZO films were enhanced by introducing a Cr buffer layer and post-annealing. The decrease in resistivity was mainly attributed to the increase in Hall mobility rather than carrier concentration. As a Cr buffer layer was inserted, the film resistivity decreased by 32% to $5.41 \times 10^{-3}\ \Omega$ cm while the energy band gap increased from 3.252 to 3.291 eV in comparison with that of the film deposited without the buffer layer. When the Cr-buffered films were annealed in a vacuum, the structural, electrical, and optical properties were improved with increasing annealing temperature. At an annealing temperature of 500 °C, the grain size, resistivity, and energy band gap attained the optimal values of 28.12 nm, $3.37 \times 10^{-3}\ \Omega$ cm and 3.357 eV, respectively. The average transmittance of TZO films in the visible region was between 75% and 84%, and it decreased with increase in the grain size. The decrease in transmittance is attributed to an increase in surface roughness due to the three-dimensional island grain growth during thermal annealing.

© 2012 Elsevier B.V. All rights reserved.

1. Introduction

Transparent conducting oxides (TCO) are extensively used in liquid crystal displays, energy efficient windows and transparent electrodes, because of their excellent electrical and optical properties [1,2]. Indium tin oxide (ITO) is the most popular commercial TCO material, but indium is toxic, rare and expensive, so the development of alternative TCO materials is essential [3]. The advantages of zinc oxide (ZnO) are low material cost, environmental friendliness, wide energy band gap (~3.3 eV) and high crystallinity, as compared to ITO films [4]. In addition, ZnO can be doped with a wide variety of ions and thus meets the demands of several fields of application. Among the various types of doped ZnO thin films, Ti-doped ZnO (TZO) films, in comparison with the ZnO films doped with Group III elements, have more than one charge valence state. When titanium atoms are doped into a ZnO lattice, they act as donors by providing two free electrons. This in turn increases the free carrier concentration and hence, decreases the resistivity. Several deposition techniques have been used to grow TCO films. Sputtering is considered to be a suitable technique for the preparation of TCO films, because it is inexpensive and offers good uniformity of deposition over large areas [5].

The properties of TZO films are generally dependent on sputtering parameters such as substrate temperature, working pressure, and ambient gas. Any changes to the resulting resistivity are responsible for changes in both the carrier concentration and the mobility, which are related to the crystallinity of the deposited doped ZnO thin films [6,7]. Chung et al. [8] indicated that the crystallinity of TZO films can be improved with a low working pressure. Lin et al. [9] investigated the effects of substrate temperatures ranging from 50 to 200 °C on the properties of sputtered TZO films and indicated that film resistivity decreased to a minimum of $9.69 \times 10^{-3}\ \Omega$ cm at 100 °C. Jiang et al. [10] and Chang et al. [11] studied the effects of annealing treatment on the properties of TZO thin films. They reported that film resistivity decreased and the average optical transmittance in the visible wavelength range changed slightly after annealing treatment. It is well known that directly depositing TCO thin films on glass substrates at low growth temperatures is difficult due to large lattice mismatch and differences in thermal expansion coefficients between the films and the substrates [12,13], resulting in poor film/substrate bonding. Inserting a buffer layer between TCO films and glass substrates is helpful for improving the bonding strength of TCO films to the substrate, which can result in stable performance of TCO films. For this

* Corresponding author. Tel.: +886 2 27867048; fax: +886 2 27867253.
E-mail address: dcwen@cc.cust.edu.tw (D.C. Wen).

0169-4332/$ – see front matter © 2012 Elsevier B.V. All rights reserved.
http://dx.doi.org/10.1016/j.apsusc.2012.06.046

Table 1
Deposition parameters of RF sputtering for TZO film and DC sputtering for a Cr buffer layer.

Parameters	RF sputtering	DC sputtering
Target	98 wt.% ZnO, 2 wt.% TiO_2 (99.995% purity)	Cr (99.95%, purity)
Sputtering power	130 W, 13.56 MHz	50 W, 30 kHz pulse frequency and 3 μs pulse time
Base pressure	5.0×10^{-6} Torr	5.0×10^{-6} Torr
Working gas	Argon (99.995%)	Argon (99.995%)
Deposition pressure	15×10^{-3} Torr	15×10^{-3} Torr
Substrate-to-target distance	85 mm	85 mm
Substrate temperature	300 °C	100 °C
Substrate rotate vertical axis	10 rpm	10 rpm
Deposition time	70 min	–

purpose, the Cr layer could be employed for adhesion enhancement because Cr has higher chemical reactivity than TCO films with glass surfaces. Moreover, Cr has a high diffusion coefficient and it can migrate quickly into TZO film during the deposition or annealing process. Thus, the existence of a Cr buffer increases the carrier concentrations and reduces the resistivity of the films. Several research groups have studied the growth of epitaxial Ga- or Al-doped ZnO thin films by introducing buffer layers, such as Al, ZnO, and SiO_2, to improve the crystalline quality and structure of the films [14–16]. However, the effect of buffer layers on the properties of TZO thin films has rarely been reported until now.

In this study, TZO thin films were deposited on Cr-buffered soda lime glass (SLG) substrates using radio frequency (RF) magnetron sputtering and then annealed in a vacuum to investigate how a buffer layer and annealing change the structure and further affect the properties of the final films. A TZO thin film was also deposited on bare SLG substrate for comparison.

2. Experimental

The TZO target was prepared by the solid state reaction method. At first, a mixture of ZnO (99.995% in purity) and TiO_2 (99.995%) powders with a composition ratio of 98:2 in wt.% was boll-milled for 20 h and pressed into a circular plate with a diameter of 50.8 mm and thickness of 3 mm, and then sintered at 1200 °C in air for 8 h.

TZO films were deposited by RF magnetron sputtering on 25 mm × 25 mm × 1.1 mm bare SLG and SLG with a Cr layer, respectively. Here, the Cr layer was coated by direct current (DC) magnetron sputtering. All samples were deposited with substrate rotation in order to attain good surface morphology. Before deposition, the targets were pre-sputtered for 5 min in order to remove any contamination. The substrates were ultrasonically cleaned with acetone and de-ionized water, and then dried under blown nitrogen gas. The RF and DC sputtering conditions are shown in Table 1.

For high transmittance, the thickness of the metal layer was not allowed to exceed a certain threshold. As the thickness of the metal layer increases, the transmittance decreases and reflection increases. Our previous study showed that the optimal thickness of an Al buffer layer is about 10 nm for AZO films [17]. Therefore, the deposition time of DC sputtering was adjusted to make sure that the thickness of the Cr buffer layer was ~10 nm. Studies show that the resistivity of TZO and AZO was improved after vacuum post-annealing at temperatures ranging from 400 to 500 °C but was decreased when annealed at 600 °C [10,18]. Hence, the deposited samples with the Cr layer were subsequently annealed in a tube furnace and evacuated to a primary vacuum level (5.0×10^{-6} Torr) at 450 and 500 °C for 20 min.

After the deposition and annealing, film structures were determined by X-ray diffraction (Rigaku-2000 X-ray diffractometer), with Cu-Kα radiation (40 kV, 30 mA and λ = 0.1541 nm) and an angle incidence of 1°. The elemental compositions of TZO target and thin films were determined by the energy dispersion spectrum (EDS) using a field emission scanning microscope

Table 2
Elemental composition of TZO target and thin film.

Sample	Ti (wt.%)	Zn (wt.%)	O (wt.%)
TZO target	2.02	79.16	18.82
TZO thin film	1.72	80.07	18.21

(FE-SEM, JEOL, JSM-6700F). The surface morphological properties were analyzed using an atomic force microscope (AFM, SPA-400). Electrical resistivity was measured by the four-point probe method (Mitsubishi chemical MCP-T600). Carrier concentration and Hall mobility were obtained from Hall-effect measurement by the van der Pauw method (Ecopia, HMS-3000). Optical transmittance was measured by a UV/VIS/IR spectrophotometer (Jasco, V-570) in the wavelength range from 300 to 800 nm. All measurements were performed at room temperature in air.

3. Results and discussion

3.1. Structural properties

The elemental compositions of TZO target and thin film are listed in Table 2. After the deposition, the Ti content decreased from 2.02 wt.% in target to 1.72 wt.% in film, whereas the Zn content increased slightly. This is consistent with the observations of Chung et al. [8]. The XRD patterns of the TZO films deposited without a buffer layer, with a buffer layer, and with a buffer layer and post-annealing at 450 and 500 °C (labeled as samples A, B, C and D) are shown in Fig. 1 All films exhibited a strong (0 0 2) peak indicating that the TZO films were highly oriented to the *c*-axis normal to the substrate [19]. Compared to sample A, the (0 0 2) peak intensity of sample B became more intense and sharper after using the Cr thin film as a buffer layer. It is indicated that the crystal quality of

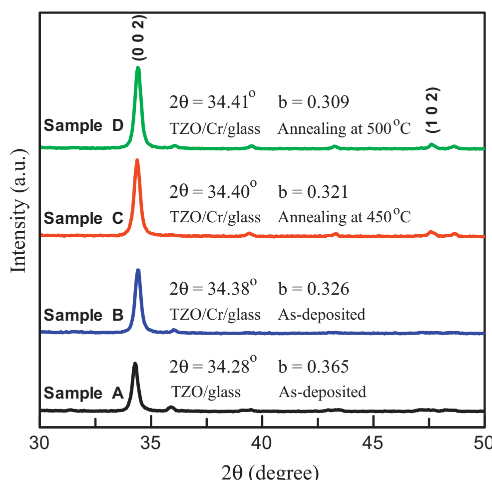

Fig. 1. XRD patterns of samples A, B, C, and D (b: full width at half maximum, FWHM).

Table 3
Position and FWHM of the (0 0 2) peak, and grain sizes of samples A, B, C, and D.

Sample condition	(0 0 2) peak position (°)	(0 0 2) FWHM	Grain size (nm)
A: TZO/glass, as-deposited	34.28	0.365	23.78
B: TZO/Cr/glass, as-deposited	34.38	0.326	26.65
C: TZO/Cr/glass, annealing at 450 °C	34.40	0.321	27.05
D: TZO/Cr/glass, annealing at 500 °C	34.41	0.309	28.12

the TZO thin film improves with the addition of the Cr buffer layer. After annealing, the intensity of the (0 0 2) peak further increases and its full width at half maximum (FWHM) also becomes more narrowed than those of sample B, revealing that better film crystallinity quality was obtained by thermal annealing. As can be seen, weak peaks of (1 0 2) orientation are observed in samples C and D. These may have developed after annealing. It is assumed that (1 0 2) orientation has higher surface energy than (0 0 2) orientation and needs more thermal energy to develop [20]. This result indicates that preferred orientation changes with a few grains in the film and the structure of TZO film becomes more random.

The FWHM of the (0 0 2) peak was narrowed from 0.365 (sample A) to 0.326 (sample B), 0.321 (sample C), and 0.309 (sample D). The corresponding average grain sizes (estimated by Scherrer's formula) were 23.78, 26.65, 27.05, and 28.12 nm, respectively. The grain size of the final film was increased by using a buffer layer and annealing. The position of the (0 0 2) peak was shifted from 34.28° (sample A) to 34.38° (sample B) when applying the Cr buffer layer. Effects of both Ti atoms substituted into Zn sites and lattice mismatch between the films and the substrate led to compressive stress in the lattice of TZO films in a direction parallel to the surface of the substrate, which could affect the lattice spacing perpendicular to the surface and, hence the (0 0 2) peak position of sample A changed to a lower diffraction angle than that of the ZnO bulk position (~34.45°). As the Cr buffer layer was inserted, the strain in the TZO film was relaxed. As a result, the position of the (0 0 2) peak was shifted to a higher angle. However, this shift was unobvious for samples C and D, as compared to sample B. It is supposed that the defects induced by the lattice mismatch and thermal expansion coefficient can get thermal energy from annealing treatment and move to the film surface. Therefore, the strain in the film is effectively relaxed. However, the buffer layer in TZO films can preclude this kind of movement and confine most of the defects in itself. Thus, the position of the (0 0 2) peak was almost unchanged for the samples C and D, after thermal annealing at 450 and 500 °C, respectively. The position and FWHM of the (0 0 2) peak and grain size of samples A, B, C, and D are summarized in Table 3. As can be seen, the (0 0 2) peak of the TZO films for samples B, C, and D becomes sharper and the peak position shifts slightly to higher values when compared with sample A, which indicates that the grain grows and less stress remains in the films after annealing. Therefore, introducing a Cr buffer layer and thermal annealing can be an effective method for improving the crystallinity of TZO films.

Fig. 2 shows AFM images of TZO film for samples A, B, C, and D. When the film was deposited without a buffer layer (sample A), some hillocks obviously occurred, as displayed in Fig. 2(a), since the film tended to be porous and loose. Ohring [21] has proposed that local mass flux divergences exist throughout film due to varying grain size and distribution. When atoms come into a grain more than leave it, the pileup or growth of the mass can be expected. Fig. 2(b) shows that the morphology of the film deposited with buffer layer (sample B) was in the shape of cobblestone and an island. This indicates that growth has taken place by nucleation and a coalescence process during the deposition of TZO film by sputtering onto Cr-buffered substrates. Randomly distributed nuclei may first form and these nuclei may then grow to form observable islands. When the TZO films were annealed at 450 and 500 °C (samples C and D), the islands come closer to each other. The larger ones appeared to grow by coalescence of the smaller ones. Thus, the surface structure of films became denser and the grains grew into larger, as shown in Fig. 2(c) and (d). Comparing these pictures with the results calculated by Scherrer's formula, it is noteworthy that the characteristic sizes obtained from AFM and XRD analysis are in agreement.

Surface roughness (Ra) was also calculated from AFM. It can be seen that the surface roughness of the TZO films was related to that of the underlying Cr layer and annealing treatment. The Ra value of TZO films deposited without and with a Cr buffer layer is 4.224 and 12.110 nm, respectively. A relatively large Ra value appeared for the TZO film deposited on the Cr-buffered substrate. Pre-deposition of a Cr buffer layer increased the surface roughness of the substrate, resulting in the increase of the Ra value of the TZO films. The Ra value increased to 13.576 nm when the TZO films were annealed at 450 °C. As the temperature further increased to 500 °C, the surface of the TZO films became rougher. Ra values of the TZO films increased with increasing temperature due to the three-dimensional island growth during thermal annealing.

3.2. Electrical properties

The resistivity (ρ), Hall mobility (μ) and carrier concentration (n) of TZO film for samples A, B, C, and D are shown in Fig. 3. As the Cr buffer layer was inserted, the film resistivity decreased from 7.98×10^{-3} Ω cm in sample A to 5.41×10^{-3} Ω cm in sample B (or a reduction of 32%). Meanwhile, the Hall mobility increased from 3.29 to 4.81 cm^2/V s and the carrier concentration increased from 1.59×10^{20} cm^{-3} to 2.93×10^{20} cm^{-3}. According to the formula of resistivity $\rho = 1/(ne\mu)$, the resistivity is a combined result of both the Hall mobility and the carrier concentration. When the TZO films were prepared with a Cr buffer layer, the grain size increased from 23.78 nm to 26.65 nm. Larger grain size can reduce grain boundary scattering and increase carrier lifetime, thus leading to an increase in conductivity due to an increase in Hall mobility and carrier concentration [22]; as a result, the electrical resistivity of TZO films decreases. When the TZO/Cr/glass films were annealed at 450 (sample C) and 500 °C (sample D), the carrier concentration showed a slight increase but the Hall mobility increased continuously, and the resistivity further was decreased by 26 and 38% to 3.98×10^{-3} Ω cm and 3.37×10^{-3} Ω cm, respectively. A possible reason is that the annealing process has the effect of increasing the grain size and crystallinity of the film, as mentioned above. This results in less grain boundary scattering. On the other hand, loss of oxygen from the crystal will also produce the interstitial zinc atoms which results in $Zn_{1+x}O$ in the matrix according to the reaction:

$$ZnO + O_o = Zn_i^* + e + 2^{-1}O_2(g) \quad (1)$$

This means that the intrinsic donor can be increased by the vacuum annealing process and thus, increase the conductivity [23]. However, Na atoms in SLG are very active at high temperatures and easily diffused into films during annealing. If a Na atom substitutes a zinc atom, it will become an acceptor, resulting in a decrease of carrier concentration [24]. Although a Cr buffer layer could prevent the diffusion of Na atoms into film, if annealing temperature is high, some Na atoms could be still diffused into TZO film through the Cr layer, lowering the carrier concentration in TZO films. Thus, the Hall mobility continues to increase when the carrier concentration exhibits a little variation after annealing. This implies that the decrease in resistivity was mainly attributed to an increase of Hall mobility rather than carrier concentration, as the films were annealed.

As described above, the decrease of resistivity roughly increased with grain size in our study. Since TZO film prepared with a Cr buffer

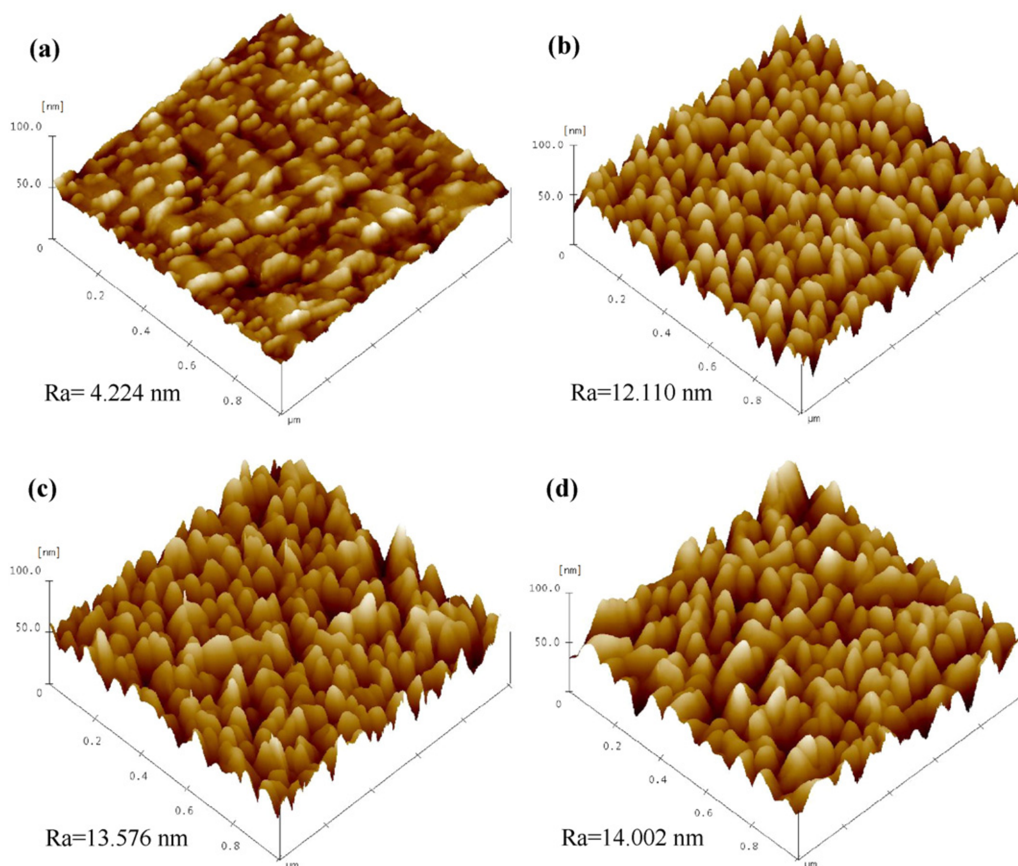

Fig. 2. AFM micrographs and surface roughness of (a) sample A: as-deposited without buffered, (b) sample B: as-deposited with Cr-buffered, (c) sample C: deposited with Cr-buffered and annealed at 450 °C and (d) sample D: deposited with Cr-buffered and annealed at 500 °C.

layer can get larger grains and can suppress the diffusion of Na atoms from SLG substrate into films, therefore, it can be concluded that the improvement of the crystallinity at an early stage of the film deposition is useful for obtaining lower resistivity in transparent conducting TZO thin films.

3.3. Optical properties

The transmittance spectra as a function of wavelengths in the range between 300 and 800 nm for samples A, B, C, and D are shown in Fig. 4. The average transmittance in the visible region is more than 75% for all samples, but the transmission in the UV–near visible region decreased abruptly. When the films were deposited with the buffer layer and for those annealed at 450 and 500 °C, the optical absorption edge shifted toward the shorter wavelength region but the average transmittance became lower, as compared to the as-deposited film without a buffer layer. In this study, in addition to the grain growth of TZO films, introducing a buffer layer and annealing also led to an increase in surface roughness due to the three-dimensional island growth. This phenomenon causes the formation of micro voids between the grain boundaries. Hence the scattering probability of incident light by micro voids existing in the films increases and we can observe a lower transmittance in the range of visible light. As a result, the average transmittance monotonically decreased from 83.95% to 75.21% with the increase of Ra value from 4.224 nm to 14.002 nm.

Since ZnO films are direct transition type semiconductors, the energy band gap (E_g) can be estimated by plotting α^2 versus hv

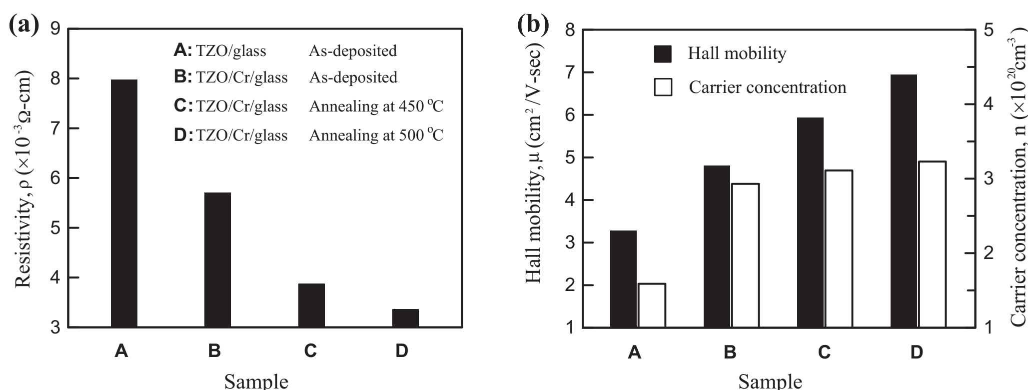

Fig. 3. (a) Resistivity and (b) Hall mobility and carrier concentration of samples A, B, C, and D.

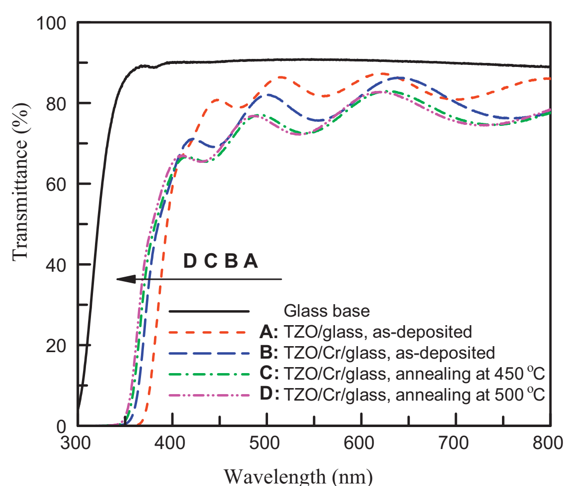

Fig. 4. Optical transmittance spectra of samples A, B, C, and D.

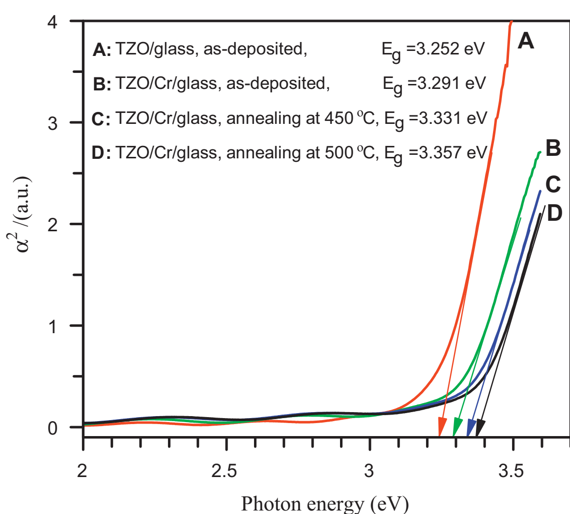

Fig. 5. Plots of α^2 versus $h\nu$ for samples A, B, C, and D.

(where α is the optical absorption and $h\nu$ is the photon energy), and then extrapolating the straight-line part of the plot to the photon energy axis. Fig. 5 shows the variation of the energy band gap for the four samples. By comparing with the film deposited without a buffer layer, inserting a Cr buffer layer and annealing at 450 and 500 °C leads to energy band gap shifts from 3.252 to 3.291, 3.331, and 3.357 eV, respectively. The energy band gap of TZO films broadens owing to an increase in the carrier concentration. This phenomenon is known as the Burstein–Moss shift [25]. Because a Cr buffer layer could prevent the diffusion of Na atoms into TZO films and provide more free electrons by the diffusion of Cr atoms from itself, the carrier concentration in the annealed samples are slight higher compared with the as-deposited film as shown in Fig. 3(b). Thus the energy band gap increased with increasing annealing temperature.

4. Conclusions

The influence of Cr buffer layers and post-annealing on the structural, electrical and optical properties of TZO films deposited on SLG substrates has been investigated. All films exhibited strong (0 0 2) diffraction peaks of hexagonal wurtzite structure. As a Cr buffer layer was inserted, the crystallinity was improved and the grain size became larger, Hall mobility and carrier concentration were also enhanced due to suppression of diffusion of Na atoms into films. The film resistivity decreased by 32% to $5.41 \times 10^{-3}\ \Omega$ cm while the energy band gap increased from 3.252 eV to 3.291 eV in comparison with that of the film deposited without a buffer layer. Post-annealing further improved the properties of TZO films due to the decrease of grain boundary scattering. The electrical and optical properties were improved with increasing annealing temperature to 500 °C, a lowest resistivity of $3.37 \times 10^{-3}\ \Omega$ cm and a maximum energy band gap of 3.357 eV were obtained. In addition, surface roughness of TZO films increased with grain size due to the three-dimensional island growth during thermal annealing. This result led to average transmittance of annealed films in the visible region which were lower than the as-deposited film with lower surface roughness.

References

[1] J. Lee, J. Metson, P.J. Evans, R. Kinsey, D. Bhattacharyya, Applied Surface Science 253 (2007) 4317.
[2] B.D. Ahn, S.H. Oh, C.H. Lee, G.H. Kim, H.J. Kim, S.Y. Lee, Journal of Crystal Growth 309 (2007) 128.
[3] T. Minami, S. Ida, T. Miyata, Y. Minamino, Thin Solid Films 445 (2003) 268.
[4] L.W. Lai, C.T. Lee, Materials Chemistry and Physics 110 (2008) 393.
[5] Y.M. Lu, C.M. Chang, S.-I. Tsai, T.S. Wey, Thin Solid Films 447–448 (2004) 56.
[6] T. Minami, H. Nanto, H. Sato, S. Takata, Thin Solid Films 164 (1988) 275.
[7] T. Minami, H. Sato, H. Imamoto, S. Takata, Japanese Journal of Applied Physics 31 (1992) L257.
[8] J.L. Chung, J.C. Chen, C.J. Tseng, Applied Surface Science 254 (2008) 2615.
[9] S.S. Lin, J.L. Huang, D.F. Lii, Materials Chemistry and Physics 90 (2005) 22.
[10] M. Jiang, X. Liu, G. Chen, J. Cheng, X. Zhou, Journal of Materials Science: Materials in Electronics 20 (2009) 1225.
[11] H.P. Chang, F.H. Wang, J.C. Chao, C.C. Huang, H.W. Liu, Current Applied Physics 11 (2011) S185.
[12] S.W. Shin, Y.B. Kwon, A.V. Moholkar, G.S. Heo, I.O. Jung, J.H. Moon, J.H. Kim, J.Y. Lee, Journal of Crystal Growth 322 (2011) 45.
[13] K.H. Bang, D.K. Hwang, J.M. Myoung, Applied Surface Science 207 (2003) 359.
[14] C.Y. Hsu, C.H. Tsang, Solar Energy Materials and Solar Cells 92 (2008) 530.
[15] T.H. Kim, S.H. Heong, B.T. Lee, Journal of Physics D 39 (2006) 957.
[16] K.H. Ri, Y.B. Wang, W.L. Zhou, J.X. Gao, X.J. Wang, J. Yu, Applied Surface Science 257 (2011) 5471.
[17] J.Y. Kao, C.Y. Hsu, G.C. Chen, D.C. Wen, Journal of Materials Science: Materials in Electronics 23 (2012) 1352.
[18] C.Y. Hsu, Y.C. Lin, L.M. Kao, Y.C. Lin, Materials Chemistry and Physics 124 (2010) 330.
[19] F.H. Wang, H.P. Chang, J.C. Chao, Thin Solid Films 519 (2011) 5178.
[20] H.S. Kang, J.S. Kang, J.W. Kim, S.Y. Lee, Journal of Applied Physics 95 (2004) 124.
[21] M. Ohring, The Materials Science of Thin Films, Academic Press, San Diego, CA, 1991, p. 379.
[22] M. Lv, X. Xiu, Z. Pang, Y. Dai, S. Han, Applied Surface Science 252 (2006) 5687.
[23] G.J. Fang, D.J. Li, B.L. Yao, Vacuum 68 (2003) 363.
[24] X.D. Zhang, H.B. Fan, J. Sun, Y. Zhao, Physica E 39 (2007) 267.
[25] K.E. Lee, M. Wang, E.J. Kim, S.H. Hahn, Current Applied Physics 9 (2009) 683.